iScience, Volume *24*

Supplemental information

Myeloid cell subsets that express latency-associated peptide promote cancer growth by modulating T cells

Galina Gabriely, Duanduan Ma, Shafiuddin Siddiqui, Linqing Sun, Nathaniel P. Skillin, Hadi Abou-El-Hassan, Thais G. Moreira, Dustin Donnelly, Andre P. da Cunha, Mai Fujiwara, Lena R. Walton, Amee Patel, Rajesh Krishnan, Stuart S. Levine, Brian C. Healy, Rafael M. Rezende, Gopal Murugaiyan, and Howard L. Weiner

Supplemental Information

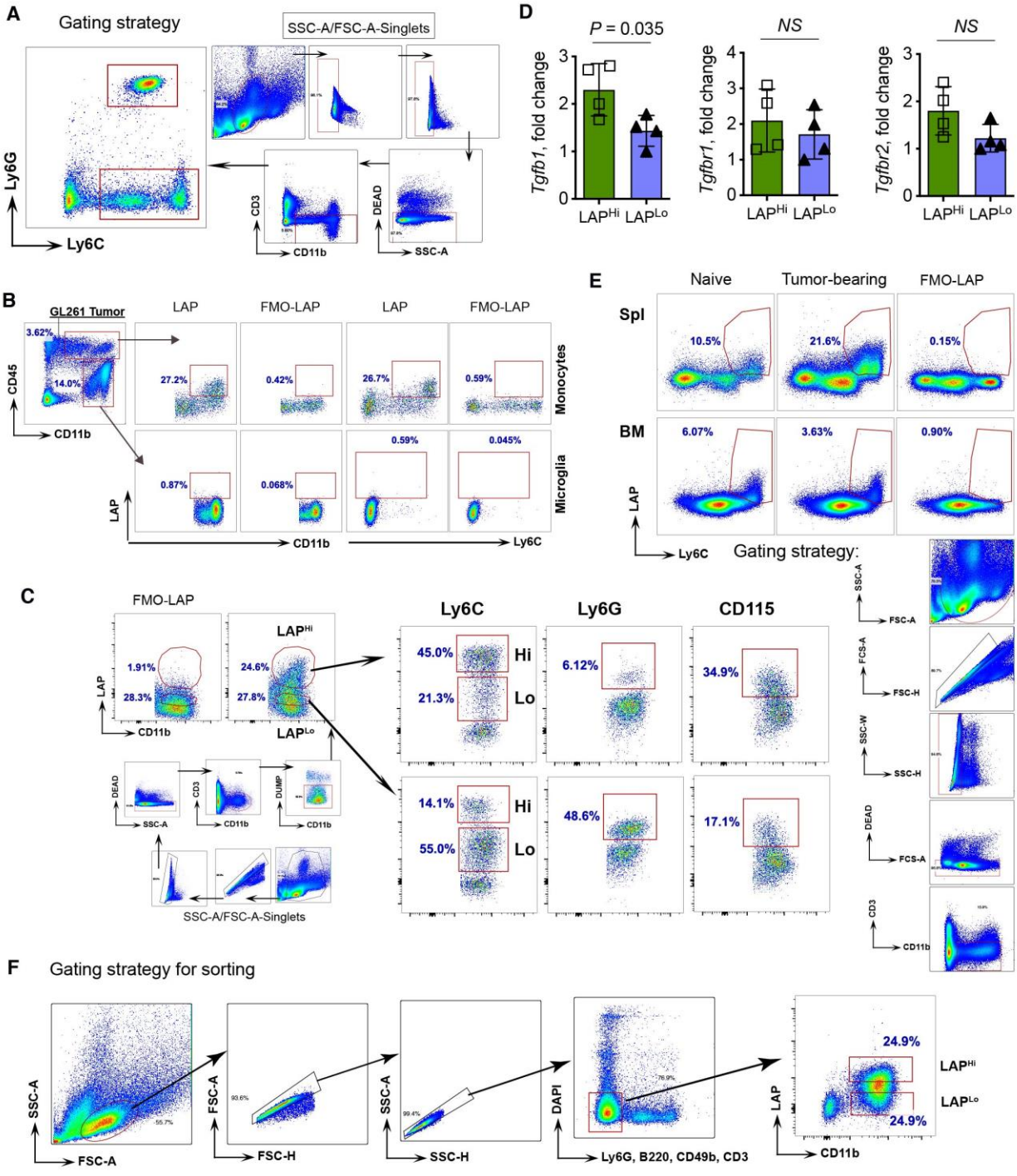

Figure S1. LAP expression on myeloid cells, related to Figure 1. (A) Spleens of CT26 tumor-bearing mice were dissociated, and cells were analyzed by flow cytometry. Ancestry gating strategy for Fig.1A (left panels) is shown. **(B)** Intracranial GL261 tumor tissue was dissociated, and LAP expression on monocytes and microglia was analyzed by flow cytometry. Gating strategy for representative FACS plots and fluorescence minus one (FMO) controls are shown. **(C)** Gating

strategy for representative FACS plots and LAP-FMO control for Fig. 1B are shown. **(D)** Analysis of mRNA expression in LAP^{Hi} vs LAP^{Lo} MCs isolated from tumor tissue of MC38 tumor-bearing mice by qPCR (n=4). **(E)** Modulation of LAP^{Hi} and LAP^{Lo} MCs in the spleen and BM of MC38 tumor-bearing mice. Representative flow cytometry dot plots with cell frequencies and gating strategy are shown. Quantification is shown in Fig. 1D. **(F)** Monocytes were isolated form spleen by EasySep Mouse Monocyte Isolation Kit (StemCell Technologies). LAP^{Hi} and LAP^{Lo} MCs were sorted by FACS following shown gating strategy. Data shown as mean $\pm$ SEM. Two-tailed t test was used for P value calculation.

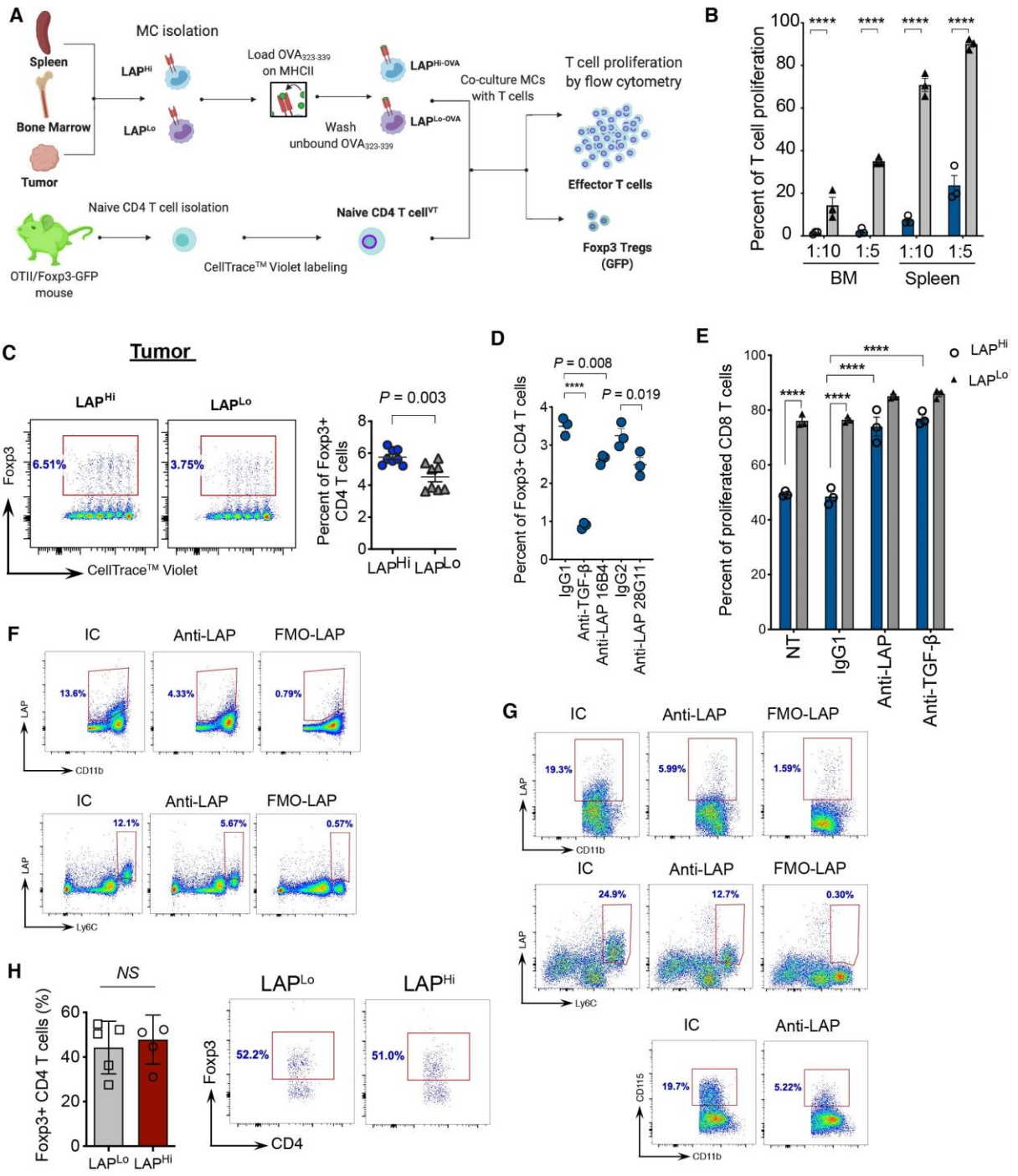

Figure S2. *In vitro* function of LAP^{Hi} MCs, related to Figure 2. (A) Schematic illustration of the *in vitro* T cell proliferation assay. Created with BioRender.com. **(B)** T cell proliferation assay of naïve CD4$^+$ T cells from OTII-Foxp3/GFP mice in the presence of LAP^{Hi} vs LAP^{Lo} MCs from spleens and bone marrow (BM) of naive WT mice. T cells were stimulated with OVA$_{323-339}$. Percent of proliferation of responder CD4$^+$ T cells is shown (n=3). **(C)** Foxp3$^+$ Treg induction was measured in the proliferation assay of responder CD4$^+$ T cells in the presence of LAP^{Hi} vs LAP^{Lo} MCs isolated from MC38 tumor. T cells were stimulated with anti-CD3. Representative dot plots

(left panel) and quantification (right panel) are shown (n=8). **(D)** $Foxp3^+$ Treg induction on CD4 T cells in the presence of LAP^{Hi} vs LAP^{Lo} myeloid cells isolated from MC38 tumor; non-treated (NT) or treated with anti-TGF-β, anti-LAP, or IgG1 and IgG2 control antibodies. T cells were stimulated with $OVA_{323-339}$. Percent of $Foxp3^+$ T cells is shown (n=3). **(E)** $CD8^+$ T cell proliferation assay in the presence of LAP^{Hi} vs LAP^{Lo} MCs isolated from spleen; non-treated (NT) or treated with anti-TGF-β, anti-LAP, or IgG1 control antibodies. T cells were stimulated with anti-CD3. Percent of proliferation is shown (n=3). **(F)** Effect of anti-LAP antibody treatment on myeloid cells (CT26 model). Mice were treated with anti-LAP or IC antibodies and frequencies of cells in the spleen measured by flow cytometry. Gating strategy for representative FACS plots and LAP-FMO control for Fig. 3A are shown. **(G)** Effect of anti-LAP antibody treatment on myeloid cells (MC38 model). Mice were treated with anti-LAP or IC antibodies and frequencies of cells in the spleen measured by flow cytometry. Gating strategy for representative FACS plots and LAP-FMO control for Fig. 3B are shown. **(H)** $Foxp3^+$ Tregs measured in the tumor tissue of mice transferred with LAP^{Lo} or LAP^{Hi} MCs. Gating strategy for representative FACS plots and quantification are shown. Data shown as mean ± SEM. Two-tailed t test (B, C), one-way ANOVA (D) and two-way ANOVA (E) were used for P value calculations.

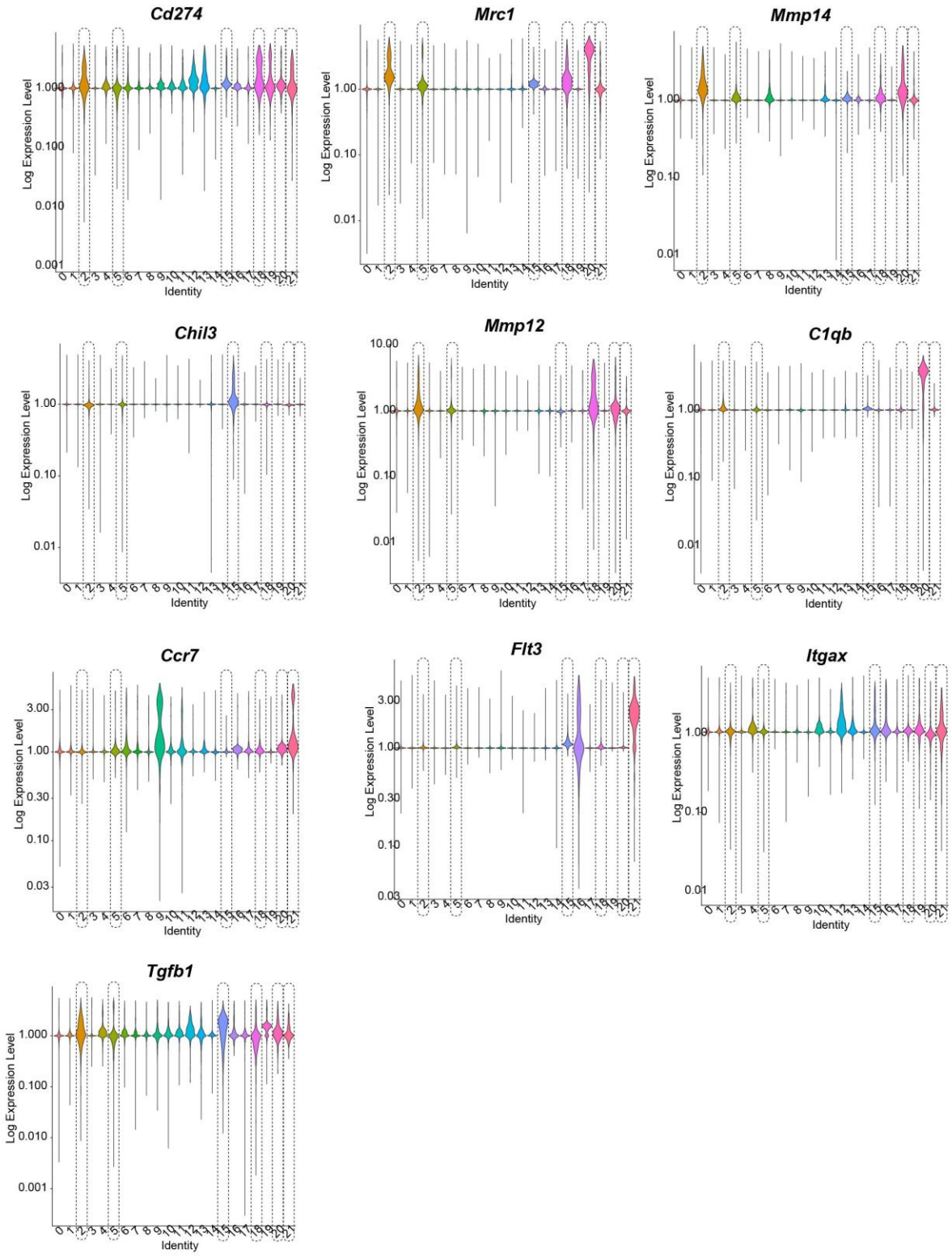

Figure S3. Violin plots based on scRNA-Seq data analysis, related to Figure 5. Violin plots show expression of markers in all clusters.

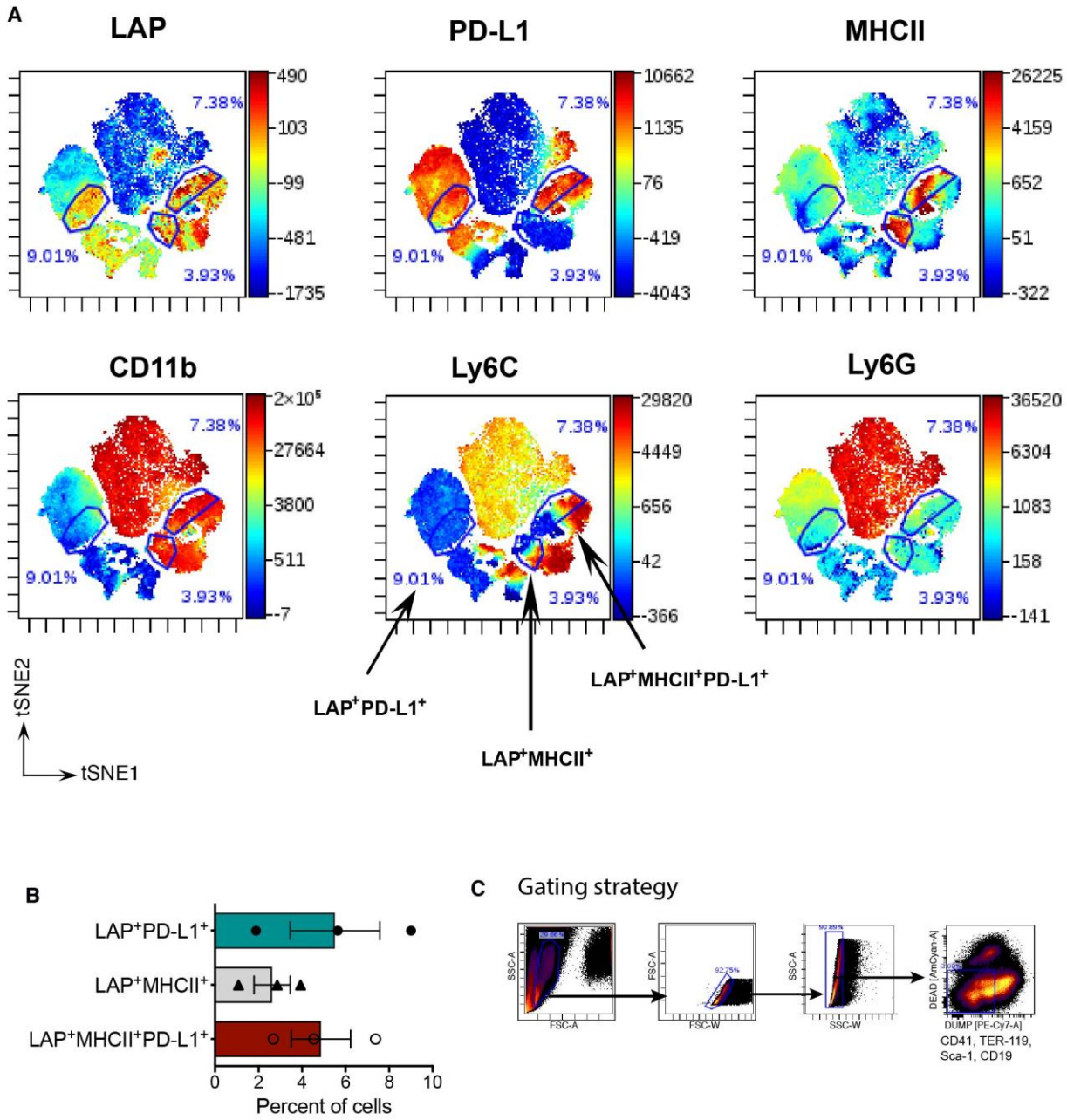

Figure S4. Co-expression of LAP with MHCII and PD-L1 in myeloid cells, related to Figure 5. (A) Flow cytometry was performed on samples from MC38 tumor, and data visualized using viSNE algorithm via Cytobank (Amir el et al., 2013; Kotecha et al., 2010). Representative viSNE plots show expression of indicated proteins. Sub-populations of $LAP^{+}PD\text{-}L1^{+}$, $LAP^{+}MHCII^{+}$ and $LAP^{+}MHCII^{+}PD\text{-}L1^{+}$ cells are highlighted with arrows. **(B)** Percent of indicated sub-populations of cells from (A) is shown (n=3). **(C)** Gating strategy for cell population used for viSNE analysis. Data shown as mean ± SEM.

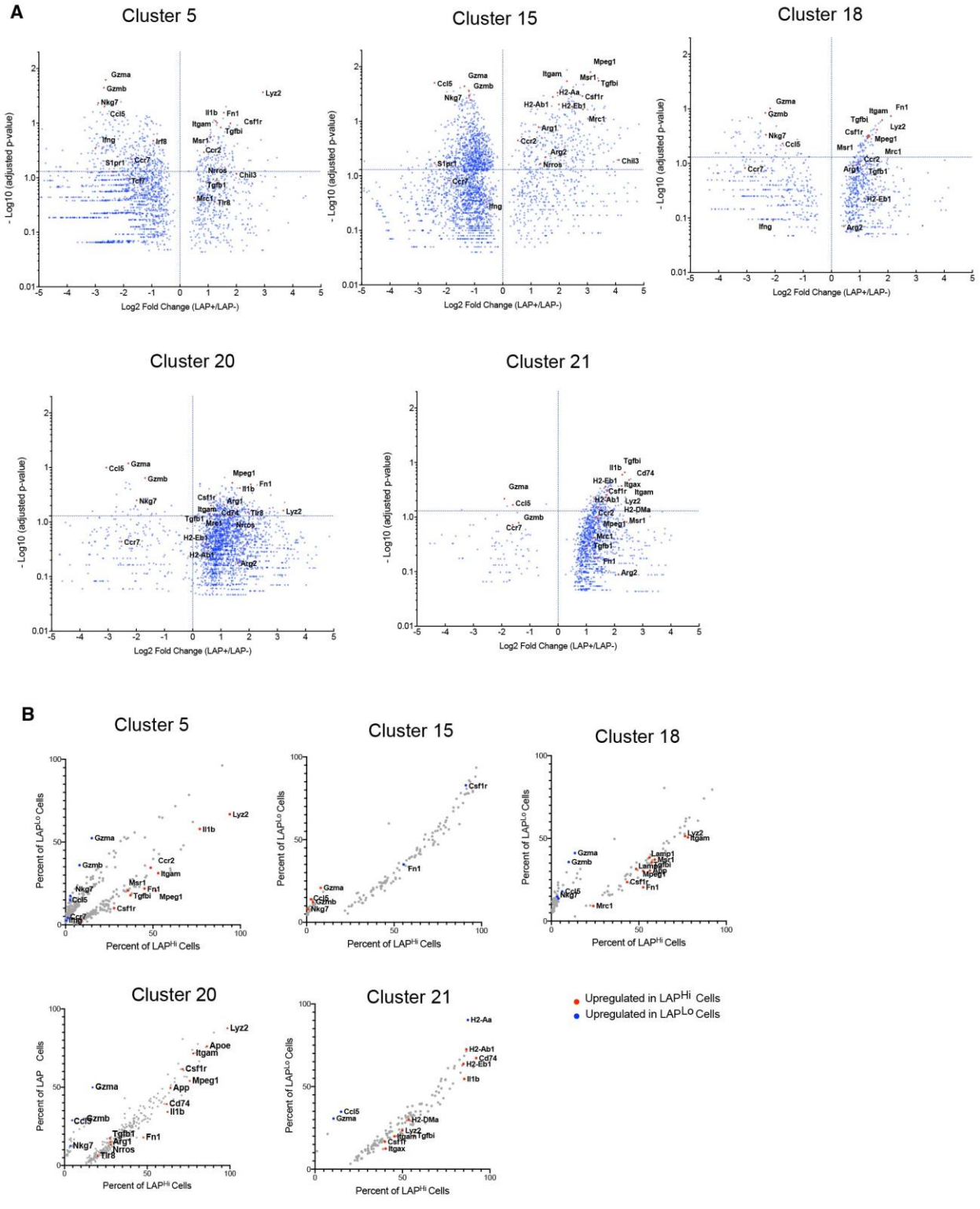
A
Cluster 5
Cluster 15
Cluster 18
Cluster 20
Cluster 21
- Log10 (adjusted p-value)
Log2 Fold Change (LAP+/LAP-)
B
Percent of LAPLo Cells
Percent of LAPHi Cells
Upregulated in LAPHi Cells
Upregulated in LAPLo Cells

Figure S5. Differential gene expression in individual clusters identified through scRNA-Seq analysis, related to Figure 5. (A) Fold change and adjusted P value plots demonstrating differential gene expression between LAP^{Hi} vs LAP^{Lo} cells in indicated clusters. **(B)** Percent of cells expressing genes which is significantly higher in LAP^{Hi} and LAP^{Lo} cells in indicated clusters. Key genes are highlighted.

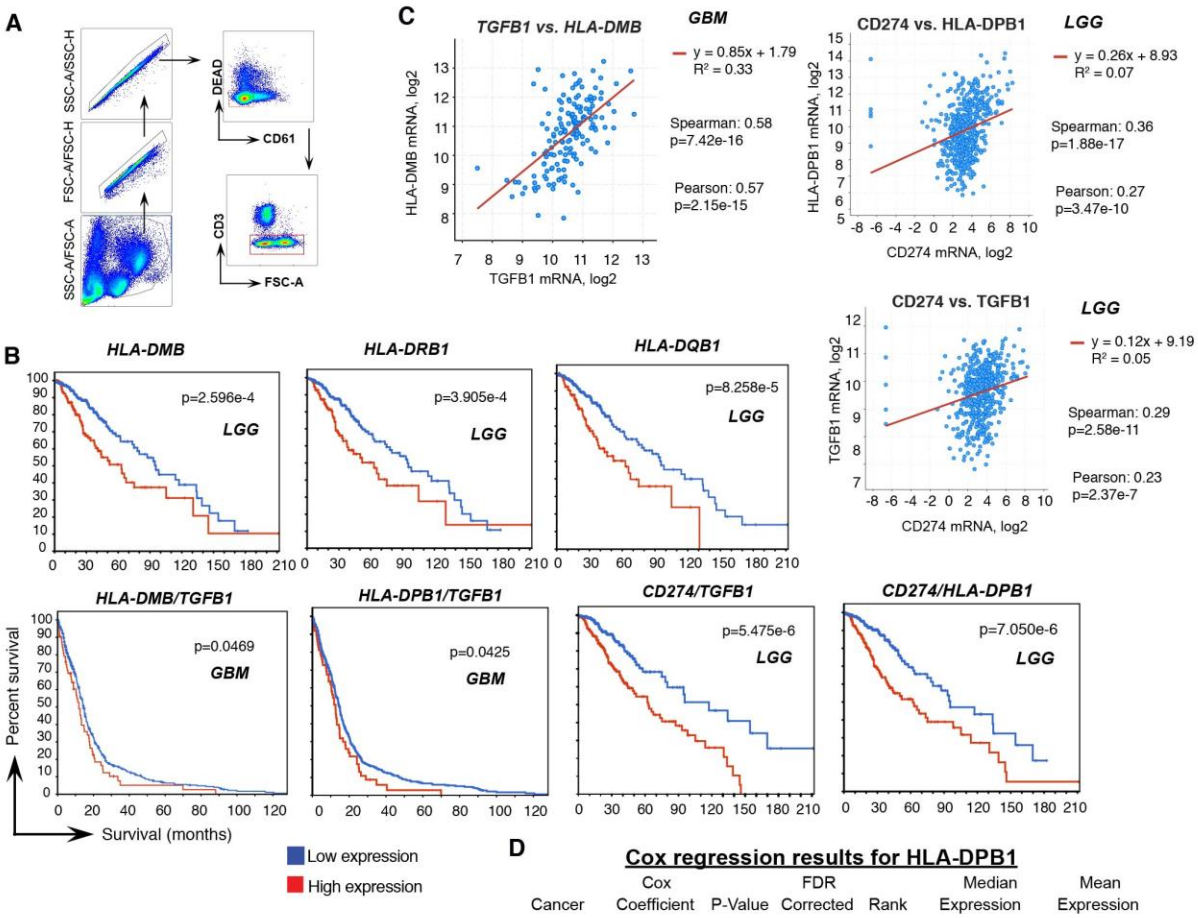

D

Cox regression results for HLA-DPB1

Cancer	Cox Coefficient	FDR P-Value	FDR Corrected	Rank	Median Expression	Mean Expression
➤ LGG	0.406	4.90e-05	2.85e-04	2888	886.22	1718.19
LAML	0.145	1.80e-01	5.76e-01	4651	2449.35	3526.66
➤ GBM	0.118	2.30e-01	8.56e-01	4428	2612.43	3380.72
LUSC	0.077	2.60e-01	7.51e-01	5785	2706.96	3804.61
READ	0.074	7.20e-01	9.82e-01	12019	1135.86	1728.65
➤ COAD	0.033	7.40e-01	9.17e-01	13178	1461.64	2204.29
ESCA	0.027	8.50e-01	9.90e-01	14365	980.14	1816.98
STAD	-0.039	6.50e-01	8.85e-01	12347	2591.9	3934.26
PAAD	-0.056	6.00e-01	7.65e-01	13459	4946.37	5487.57
OV	-0.071	3.50e-01	8.39e-01	6955	2639.49	3640.33
BLCA	-0.073	3.20e-01	5.85e-01	8874	1527.21	3196.52
HNSC	-0.115	1.10e-01	4.27e-01	4159	2286.22	3468.55
UCEC	-0.136	2.10e-01	9.81e-01	3444	2242.75	3366.8
LIHC	-0.175	6.20e-02	2.47e-01	3960	1855.83	2904.53
KIRC	-0.184	1.70e-02	4.73e-02	5949	8029.32	9411.85
BRCA	-0.218	1.50e-02	2.57e-01	948	3166.61	4039.74
LUAD	-0.262	3.80e-04	1.67e-02	379	6217.8	7780.33
KIRP	-0.275	6.80e-02	1.82e-01	6113	3374.85	4745.86
CESC	-0.278	2.80e-02	2.57e-01	1757	2895.8	4409.03
SARC	-0.285	8.50e-03	9.52e-02	1445	3103.22	6283.42
SKCM	-0.358	2.30e-07	8.21e-05	45	3117.18	5914.74

Figure S6. LAP expression in cancer patients, related to Figure 6. (A) Gating strategy for LAP expression on $MHCII^+$ cells (Fig. 6C). **(B)** Percent survival of patients with relatively high or low mRNA expression of indicated genes, including MHCII genes (*HLA-DMB, HLA-DRB*1, *HLA-DQB1*) and combined expression of MHCII (*HLA-DPB1, HLA-DMB*), PD-L1 (*CD274*), and/or LAP (*TGFB1*) genes, in the tumor tissue of glioma (LGG and GBM) patients. Graphs and P values were downloaded from TCGA dataset via cBioPortal (https://www.cbioportal.org; (Cerami et al., 2012; Gao et al., 2013)). **(C)** Correlation between *TGFB1* and *HLA-DMB, CD274* and *HLA-DPB1, CD274* and *TGFB1* expression in the tumor tissue of glioma patients (https://www.cbioportal.org; (Cerami et al., 2012; Gao et al., 2013)). **(D)** Cox regression results for *HLA-DPB1* in 21 cancer patients. Arrows indicate positions of LGG, GBM, and COAD (colon adenocarcinoma). Dashed line divides samples with positive vs negative Cox coefficients. Table was downloaded directly from the OncoLnc portal (http://www.oncolnc.org; (Anaya, 2016)) after ranking cancer types based on the Cox coefficient (from high to low).

Table S1. TaqMan qPCR primers, related to STAR Methods.

TaqMan qPCR Probes	SOURCE	IDENTIFIER/Cat# 4331182
B2m	ThermoFisher	Assay ID: Mm00437762_m1
Ccl5	ThermoFisher	Assay ID: Mm01302427_m1
Ccr2	ThermoFisher	Assay ID: Mm01216173_m1
Gapdh	ThermoFisher	Assay ID: Mm99999915_g1
H2-Ab1	ThermoFisher	Assay ID: Mm00439216_m1
H2-Eb1	ThermoFisher	Assay ID: Mm00439221_m1
Ifng	ThermoFisher	Assay ID: Mm01168134_m1
Il10	ThermoFisher	Assay ID: Mm01288386_m1
Il12a	ThermoFisher	Assay ID: Mm00434169_m1
Mrc1	ThermoFisher	Assay ID: Mm01329362_m1
Msr1	ThermoFisher	Assay ID: Mm00446214_m1
Lrrc33	ThermoFisher	Assay ID: Mm00524817_m1
Stat3	ThermoFisher	Assay ID: Mm01219775_m1
Tgfb1	ThermoFisher	Assay ID: Mm01178820_m1
Tgfbr1	ThermoFisher	Assay ID: Mm00436964_m1
Tgfbr2	ThermoFisher	Assay ID: Mm00436976_m1